

BRIDGE DAMAGE ASSESSMENT USING SINGLE POST-EVENT TERRASAR-X IMAGE

Wen Liu and Fumio Yamazaki

Graduate School of Engineering, Chiba University, Japan.

ABSTRACT

Due to the huge tsunamis occurred in the 2011 Tohoku-Oki, Japan, earthquake, more than 100 bridges located in the Pacific coast of the Tohoku region were severely damaged. In this study, the extraction of the damaged bridges in Miyagi Prefecture, Japan, was conducted by two methods using two post-event TerraSAR-X (TSX) intensity images, respectively. First, the statistical features within the outlines of the target bridges were calculated. The thresholding method of the backscatter intensity was applied to extract the damaged bridges. Then the TSX image was transformed into a binary image including water and non-water regions. The percentages of no-water regions within the bridge outlines were used to classify the washed-away and survived bridges. By comparing with the optical images and the report of field surveys, the accuracies of the proposed two methods and the influence of the shooting date were investigated.

Index Terms— the 2011 Tohoku-Oki, Japan, earthquake, washed-away bridges, backscattering intensity, GIS data, inundation

1. INTRODUCTION

Road networks are essential components of infrastructures. They are important for the emergency response after a disaster occurs. In the March 11, 2011 Tohoku-oki, Japan, earthquake and associated tsunamis, more than 100 bridges in Iwate and Miyagi Prefectures were washed away by the huge tsunamis [1]. It caused road closures in a wide area over a long time. Synthetic aperture radar (SAR), which is essentially not affected by weather and sunlight conditions, is effective in emergency response. Various damage detection methods using multi-temporal SAR images taken before and after a disaster have been proposed [2-4]. However, studies on damage detection of bridges due to earthquakes or tsunamis from SAR imagery are limited. In our previous studies [5-6], the backscattering model of bridges in the SAR image has been revealed. The average values of the backscatter intensity within the bridge outlines were useful for detecting washed-away bridges. In addition, comparing with the high-resolution full-polarization airborne SAR images, the TerraSAR-X (TSX) HH intensity images have enough capability to identify the damaged

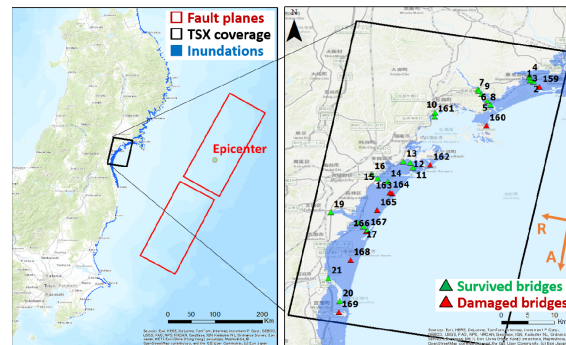


Fig. 1 Locations of the study area and target bridges in the coast of Miyagi Prefecture, Japan

bridges. Our previous studies focused on the bridges in Iwate Prefecture. In this study, the inundated bridges in Miyagi Prefecture were investigated using two post-event TSX intensity images.

2. STUDY AREA AND IMAGERY DATA

The study area was set in Miyagi Prefecture, Japan, which was one of the most affected regions by the 2011 Tohoku-Oki earthquake and resultant tsunamis. A GIS dataset, including water and road boundary lines, was downloaded from the Fundamental Geospatial Data [7]. The roads over water polygons were considered as bridges and were extracted by polygons. Using the GIS data created in 2008 before the earthquake, 32 bridges located in the inundation of Pacific coast were selected as targets. Their locations are shown in Fig. 1.

11 out of the 32 target bridges were investigated by the National Institute for Land and Infrastructure Management (NILIM) [1], the detailed information of those target bridges is summarized in Table 1. The decks of the six bridges were reported as washed away. Bridge No. 160 was reported as a bridge that survived in the report of NILIM; however, parts of its embankment behind abutment were confirmed as washed away based on the aerial photos taken by GSI [8]. Bridges Nos. 162 and 169, which were judged as survived by NILIM, were blocked by a large amount of debris. Thus, those nine bridges were counted as damaged bridges. Besides the undamaged bridges Nos. 161 and 167, 21 undamaged or slightly damaged bridges located in the upstream were selected to represent the undamaged bridges.

Table 1. Detailed information of the investigated eleven bridges

No.	Length [m]	Width [m]	Height [m]	Structural type	Damage condition
159	126.00	11.75	4.06	PC T-shaped girder	Washed-away
160	45.49	6.80	2.10	PC T-shaped girder	Washed-away
161	252.00	3.00	2.10	Steel I-shaped girder	No damage
162	5.80	7.00	1.32	RC floor slab	Debris
163	34.00	6.80	0.60	Steel H-shaped girder	Washed-away
164	10.80	4.30	0.65	PC floor slab	Washed-away
165	31.90	6.80	0.62	Steel H-shaped girder	Washed-away
166	31.00	3.30	0.50	Steel I-shaped girder	Washed-away
167	26.00	7.20	2.25	RC floor slab	No damage
168	16.90	3.70	0.50	RC floor slab	Washed-away
169	238.00	4.00	2.25	PC floor slab	Debris

Two TSX intensity images taken on March 13 and April 4, 2011 (two days and 24 days after the tsunami attack), were used in this study. The images were acquired in the StripMap mode by the HH polarization. The resolutions are about 3 m. They were provided as the EEC (enhanced ellipsoid corrected) products in the 1.25-m pixel size. An Enhanced Lee filter [9] with a 3×3 pixels window was applied to reduce the speckle noises.

3. DAMAGE DETECTION OF BRIDGES

As reported in the previous research [10], the ground movements of more than 3 m occurred in the coastal area. The ground movement caused the mismatch between the created bridge outlines and the bridges in the SAR images. In addition, the layover of objects in SAR images is another reason of the mismatch. For the eleven investigated bridges, the clearance heights between the deck and water were reported as presented in **Table 1**. For the other 21 bridges, the heights are unknown. The average height of the eleven bridges was adopted as the representative height for the layover. Based on the 37.3° incident angle and the 280.0° range direction, the shifts of the layovers were 0.23 m to the east and 1.29 m to the south. The average values of the ground movements in the study area on March 13 and April 4, 2011, were also calculated. Then the movements of the bridge polygons were obtained by adding the layover length and the ground movements. Finally, the created bridge outlines were shifted 4.09 m to the east and 0.97 m to the south in the TSX image on March 13, 4.27 m to the east and 1.02 m to the south in the TSX image on April 4. The parts of the TSX images around seven bridges were extracted as samples and shown in **Fig. 2**.

3.1. Thresholding of the average backscatter coefficients

According to our previous studies [5-6], the thresholding method of the average values within the shifted bridge

polygons and the standard deviations (STD) are effective to detect the damaged bridges. Thus, they were calculated from the two post-event TSX images respectively and shown by the scatter plots in **Fig. 3**. Nine damaged bridges are shown using red triangles and the undamaged bridges are shown using green triangles. Similar to the results obtained in Iwate Prefecture [6-7], the backscatter intensity of the washed-away bridges is smaller than the undamaged bridges. Comparing the plot of March 13 to that of April 4, the average values of the undamaged bridges were almost the same whereas the average value of the damaged bridges changed much. Those changes occurred due to the proceeding recovery work.

The optimal threshold of the average value was estimated as -14.5 dB for the washed-away bridges in Iwate Prefecture [6]. However, this value was not appropriate for the case in this study. Since only part of the decks were washed-away, the average values for several damaged bridges were larger than the case in Iwate Prefecture. The best threshold value was investigated as -11.0 dB for both the post-event TSX images, when the F-score [11] of the damaged bridges achieved the maximum value. This threshold value is also plotted in **Fig. 3**. Two damaged bridges, Nos.164 and 169, were excluded by this threshold value, whereas three undamaged bridges, Nos. 10, 12 and 17, were misclassified as damaged. The error Matrix is presented in **Table 2**. The overall accuracy was 84% and the Kappa coefficient was 0.63.

The omitted damaged bridge No. 164 and the misclassified undamaged bridges Nos. 12 and 17 are shown in **Fig. 2**. Bridge No. 64 is a small bridge. Although the deck was washed away, the accumulation of debris caused a large backscattering value. Thus, it is difficult to estimate its damage using only the intensity value. The other omitted damaged bridge No. 169 had the same problem. Bridge No. 12 is an undamaged bridge with four lanes. However, the low backscattering from the wide smooth deck caused the low average value within the bridge polygon. Then it was detected as damaged. This problem also occurred in the bridge No. 10. The error of bridge No. 17 was mainly caused by the mismatching between its layover and the bridge polygon. The clearance height of bridge No. 17 is higher than the average height 0.8 m. Part of the shadow region was included in the polygon, which caused the small average value of the backscatter intensity.

3.2. Thresholding of the percentage of non-water regions

In the previous study [6], the thresholding method using the percentage of non-water regions also showed good potential to detect the washed-away bridges. This method was attempted in this study. The TSX intensity images were transformed to binary images, where the water region is 0 and the non-water region is 1. The threshold value was set according to the histogram of a coastal area including both water and urban regions. The least point on the histogram

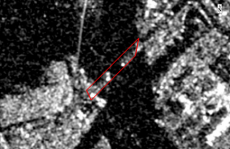
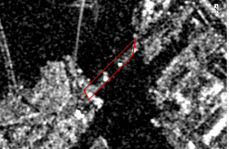


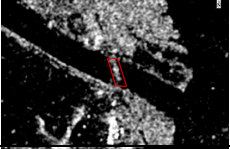
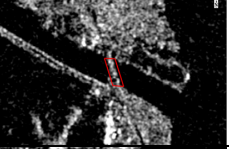


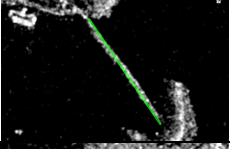
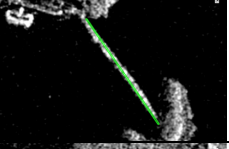


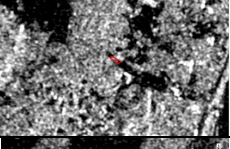
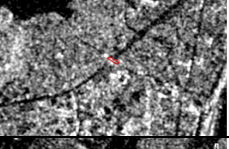


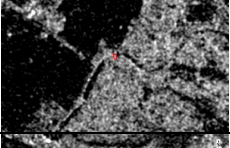
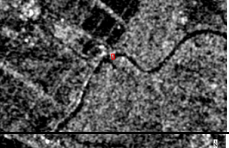


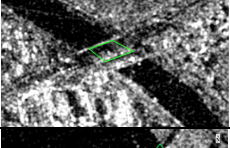
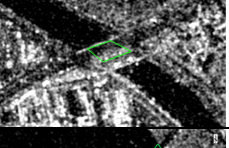


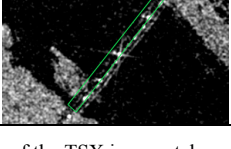
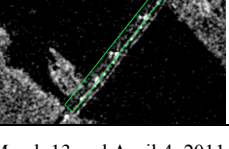

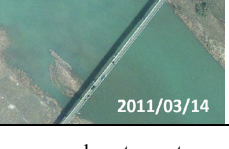
Bridge No. Condition	Post-event TSX		Pre-event optical image (Google Earth)	Post-event optical image (Google Earth)
	March 13, 2011	April 4, 2011		
159 Washed-away				
160 Washed-away				
161 No damage				
162 Debris				
164 Washed-away				
12 No damage				
17 No damage				

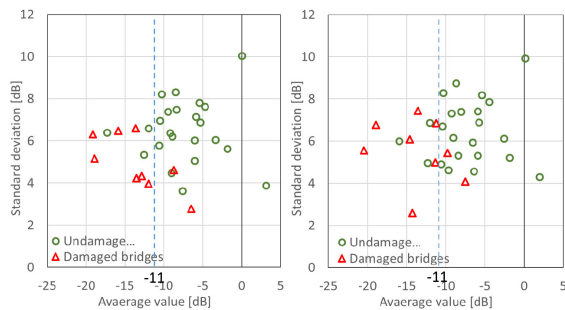
Fig. 2 Comparison of the TSX images taken on March 13 and April 4, 2011, with the shifted bridge outlines, the pre- and post-event optical images cited from Google Earth.

between two peaks of the water and non-water regions was adopted. The percentages (p) of the non-water region within the bridge outlines were calculated to classify the washed-away bridges.

In Iwate Prefecture, the thresholding value of the percentage was set as 1/3 (33%) of the polygon. However, it increased to 1/2 (50%) for the case in this study. The error matrixes for the two TSX image are presented in **Table 3**, respectively. The blocked bridges Nos. 162 and 169 were classified into survived bridges. The overall accuracy was

88% and the Kappa coefficient was 0.59 for the TSX image on March 13, whereas the overall accuracy was 91% and the Kappa coefficient was 0.71 for the TSX image on April 4, show good level of agreement.

The washed-way bridges Nos. 163, 164 and 168 could not be detected from the TSX image on March 13. The mainly reason was the accumulation of debris. The debris on the bridge No. 163 were cleared up later, thus, it could be identified from the TSX image on April 4.



(a) March 13, 2011

(b) April 4, 2011

Fig. 3 Scatter plots of the average value and the standard deviation of the backscattering coefficients within the shifted bridge polygons.

Table 2 Error matrixes using the thresholding of the backscattering coefficients of the shifted bridge polygons

$\mu < -11.0$ dB		Report of the NILIM			
		Damaged	Undamaged	Total	User Acc.
TerraSAR-X	Damaged	7	3	10	70%
	Undamaged	2	20	22	91%
	Total	9	23	32	
Producer Acc.		78%	87%		84%

Table 3 Error matrixes using the thresholding of the percentage of water and non-water regions

$p < 50\%$		Report of the NILIM			
		Washed-away	Survived	Total	User Acc.
TerraSAR-X	Washed-away	4	1	5	80%
	Survived	3	24	27	89%
	Total	7	25	32	
Producer Acc.		57%	96%		88%

$p < 50\%$		Report of the NILIM			
		Washed-away	Survived	Total	User Acc.
TerraSAR-X	Washed-away	5	1	6	83%
	Survived	2	24	26	93%
	Total	7	25	32	
Producer Acc.		71%	96%		91%

3.3. Discussions

The comparison of the results from the TSX image on March 13 and April 4 was carried out to investigate the influence of the recovery work. Using the thresholding of the average backscatter coefficients, although the backscatter intensity within the polygons of the damaged bridges changed, the accuracy was not affected. Using the thresholding of the percentage of non-water regions, the clear up of debris improved the accuracy of detecting the

washed-away bridges. This result was similar to the detection of the washed-away buildings. However, the second method was weak in detecting the part washed-away bridges and the blocked bridges.

4. CONCLUSIONS

In this study, damage assessment of 32 inundated bridges in Miyagi Prefecture, Japan, due to the 2011 Tohoku-Oki earthquake and tsunamis were carried out by two methods using two post-event TerraSAR-X intensity images taken on March 13 and April 4, 2011. Using the same thresholding value of the average backscatter coefficients, 7 out of 9 damaged bridges could be detected from both the SAR image respectively. However, the thresholding of the percentage of non-water regions showed better results using the TSX image taken on April 4, after the clear up of debris. In addition, the second method only worked for the washed-away bridges. In the future, the continuity of the strong backscatter from the fence would be considered to detect the unpassable damaged bridges.

5. ACKNOWLEDGEMENTS

The TerraSAR-X data are the property of the German Aerospace Center (DLR) and Infoterra GmbH and were made available by the PASCO Corporation.

6. REFERENCES

- [1] National Institute for Land and Infrastructure Management (NILIM), "Annual report of road-related research in FY 2013." Technical Note of NILIM, no. 843, 2013. (in Japanese)
- [2] L. Dong, and J. Shan, "A comprehensive review of earthquake-induced building damage detection with remote sensing techniques," *ISPRS Journal of Photogrammetry and Remote Sensing*, 84, pp. 85-99, 2013.
- [3] P.T.B. Brett, and R. Guida, "Earthquake damage detection in urban areas using curvilinear features," *IEEE Transactions on Geoscience and Remote Sensing*, 51(9), pp. 4877-4884, 2013.
- [4] S. Plank, "Rapid damage assessment by means of multi-temporal SAR-A comprehensive review and outlook to Sentinel-1," *Remote Sensing*, 6, pp. 4870-4906, 2014.
- [5] W. Liu, and Fumio Yamazaki, "Extraction of collapsed bridges due to the 2011 Tohoku-oki earthquake from post-event SAR images," *Journal of Disaster Research*, 13(2), pp. 281-290, 2018.
- [6] W. Liu, H. Hirano, and F. Yamazaki, "Damage Assessment of Bridges Using Post-Event High-Resolution Sar Images," *2018 IEEE International Geoscience and Remote Sensing Symposium (IGARSS)*, pp. 862-865, 2018.
- [7] Geospatial Information Authority of Japan (GSI), Fundamental Geospatial Data, <http://www.gsi.go.jp/kiban/>, 2018.
- [8] Geospatial Information Authority of Japan (GSI), Digital Map of Japan, <http://maps.gsi.go.jp/>, 2018.
- [9] A. Lopes, R. Touzi, E. Nezry, "Adaptive speckle filters and scene heterogeneity," *IEEE Transaction on Geoscience and Remote Sensing*, 28(6), pp. 992-1000, 1990.
- [10] W. Liu, and F. Yamazaki, "Detection of crustal movement from TerraSAR-X intensity images," *IEEE Geoscience and Remote Sensing Letters*, 10(1), pp. 199-203, 2013.
- [11] D.M.W. Powers, "Evaluation: From Precision, Recall and F-Measure to ROC, Informedness, Markedness & Correlation," *Journal of Machine Learning Technologies*, 2 (1), pp. 37-63, 2011.